Journal of Photochemistry & Photobiology, A: Chemistry 427 (2022) 113791

Contents lists available at ScienceDirect

Journal of Photochemistry & Photobiology, A: Chemistry

journal homepage: www.elsevier.com/locate/jphotochem

Immobilization of highly active titanium dioxide and zinc oxide hollow spheres on ceramic paper and their applicability for photocatalytic water treatment

Tamás Gyulavári [a,*], Viktória Márta [a], Zoltán Kovács [a,b], Klára Magyari [a,c], Zsolt Kása [d], Gábor Veréb [e], Zsolt Pap [a,c,f,*], Klara Hernadi [a,g]

[a] Department of Applied and Environmental Chemistry, University of Szeged, Rerrich Béla sqr. 1, Szeged H-6720, Hungary
[b] Faculty of Physics, Babes-Bolyai University, Mihail Kogălniceanu Str. 1, Cluj-Napoca RO-400084, Romania
[c] Nanostructured Materials and Bio-Nano-Interfaces Center, Interdisciplinary Research Institute on Bio-Nano-Sciences, Babes-Bolyai University, Treboniu Laurian 42, Cluj-Napoca RO-400271, Romania
[d] Material and Solution Structure Research Group, University of Szeged, Dóm sqr. 8, Szeged H-6720, Hungary
[e] Department of Biosystems Engineering, Faculty of Engineering, University of Szeged, Moszkvai blvd. 9, Szeged H-6725, Hungary
[f] Institute of Research-Development-Innovation in Applied Natural Sciences, Babes-Bolyai University, Fântânele Str. 30, Cluj-Napoca RO-400294, Romania
[g] Institute of Physical Metallurgy, Metal Forming and Nanotechnology, University of Miskolc, Miskolc-Egyetemváros, C/1 108, Miskolc H-3515, Hungary

ARTICLE INFO

Keywords:
Titanium dioxide
Zinc oxide
Hollow sphere
Immobilization
Al_2O_3-based ceramic paper
Photocatalysis

ABSTRACT

Titanium dioxide and zinc oxide hollow spheres were synthesized using carbon spheres as templates. To investigate their practical applicability, they were immobilized on ceramic paper support using titanium(IV) isopropoxide as an adhesive. The immobilization process was successful, reinforced by X-ray diffraction, scanning electron microscopy and infrared spectroscopy measurements. The photocatalytic activity of the samples was investigated by applying them in both suspended and immobilized forms. These measurements were performed under UV-A irradiation using phenol as a pollutant. To investigate reusability and stability, the photocatalytic experiments were carried out consecutively three times. After immobilization, the photocatalytic activity order observed for hollow TiO_2 and hollow ZnO was reversed. The formation of a heterojunction was deduced to be responsible for the observed photocatalytic activity. The immobilized catalysts were demonstrated to be highly reusable as they largely retained their photocatalytic activity during the repeated measurements, and no catalyst leaching was observed.

1. Introduction

Due to constant research, heterogeneous photocatalysis is gradually becoming a real alternative of conventional technologies for water purification. For this purpose, photocatalysts can be either suspended in the water to be treated or immobilized on a suitable surface. In the former case, higher photocatalytic efficiency can be reached because of more efficient mass transfer and larger contact area between catalysts and pollutants [1]. However, this approach has numerous drawbacks, such as light scattering, the formation of aggregates, and, most importantly, additional costs to recover catalyst particles [2]. The latter step is a crucial one to enable reusability, but it severely limits the industrial applicability of suspended catalysts. To overcome this problem, catalysts need to be immobilized on appropriate supports.

The characteristics and durability of immobilized catalysts are largely dependent on the support material and the method of fixing. Numerous attempts have been made to use materials such as glass [1–6], aluminum [7,8], polymers [9–11], biopolymers [12], stone [13], zeolite [14] or even ceramic paper [15–17] as supports. Regarding the method of immobilization, it can be carried out in two main ways. Premade photocatalysts can be fixed on a surface with or without adhesive materials (e.g., polyvinyl alcohol [18], SiO_2 glue [4], hydrolyzed titanium dioxide precursors [15–17]) *via* techniques such as dip coating, electrophoretic deposition or embedding into polymers [5,9–11,17,19,20]. If adhesives are used, it is important that they should prevent catalyst leaching, resist degradation, and not poison the catalysts [16,21]. Another approach is to synthesize photocatalysts in situ in the presence of support materials by methods like sol–gel processes [22] or chemical

* Corresponding authors at: Department of Applied and Environmental Chemistry, University of Szeged, Rerrich Béla sqr. 1, Szeged H-6720, Hungary (Z. Pap).
E-mail addresses: gyulavarit@chem.u-szeged.hu (T. Gyulavári), pzsolt@chem.u-szeged.hu (Z. Pap).

https://doi.org/10.1016/j.jphotochem.2022.113791
Received 25 October 2021; Received in revised form 17 December 2021; Accepted 6 January 2022
Available online 10 January 2022

vapor deposition [3]. However, the possibilities to control the properties of catalysts prepared in this way are limited.

When using premade photocatalysts immobilized on a suitable surface, it is essential that they should have a high initial photocatalytic activity. This is important both to compensate for the activity loss due to immobilization and to ensure that the photocatalysts are still efficient enough to degrade pollutants. Many attempts have been made to increase the photocatalytic activity of catalysts *via* techniques such as doping [23,24], noble metal deposition [20,25,26], sensitization with dyes [27,28], preparation of composites [9,29,30], and morphological modifications [24,26,31,32]. Withing the latter group, a relatively novel way to increase efficiency is to prepare catalysts in the form of hollow spheres, since they possess increased light-harvesting capabilities compared to solid spheres [33,34].

In this study, our goal was to fabricate TiO_2 and ZnO hollow spheres and investigate their photocatalytic activity when used in either suspended or immobilized form. Previously in our research group it has already been observed that the photocatalytic activities of hollow TiO_2 spheres were higher compared to those of solid spheres [26,35]. Veréb et al. also found that hydrolyzed titanium dioxide precursors can be used as adhesives, while ceramic paper can be used as a support to prepare immobilized photocatalysts in a facile way [17]. Accordingly, in this work, this method was applied to fix premade, highly efficient TiO_2 and ZnO hollow spheres on ceramic paper *via* spray coating. Their coverage on the support was determined not only by calculations but experimentally as well. The observed photocatalytic activities were correlated with the structural properties of the photocatalysts.

2. Experimental section

2.1. Materials

Table sugar (Magyar Cukor Zrt., Koronás^{TM}) was used as carbon source for the shape tailored synthesis. Sodium hydroxide (Molar Chemicals, a.r., 50%) was used to set the pH and acetone (Molar Chemicals, 99.96%) to purify the carbon spheres. Titanium(IV) butoxide (Sigma-Aldrich, reagent grade, 97%) and zinc acetylacetonate monohydrate (Alfa Aesar, 99.99%) were used as TiO_2 and ZnO precursors, respectively. Ethanol (Molar Chemicals, absolute ethanol) and ultrapure Millipore Milli-Q water were used as solvents. Ceramic paper produced by Cotronics Corporation (Al_2O_3-based, non-woven, 1.6 mm thickness, Catalog No.: 300-40-1) was used as a support. Titanium(IV) isopropoxide (Sigma-Aldrich, 97%) was used as an adhesive to fix the catalysts to the support, ethanol (Molar Chemicals, absolute ethanol) to wet the ceramic papers, and isopropyl alcohol (VWR, Ph. Eur. grade) to prevent the hydrolysis of the adhesive. Phenol (Spektrum 3D, analytical grade) was used for the photocatalytic activity measurements.

2.2. Synthesis

The shape tailored syntheses were carried out using carbon spheres as templates to ensure the formation of hollow spheres [26]. First, to synthesize carbon spheres, a sucrose solution (0.15 M, 180.7 mL) was prepared, and its pH was set to 12 using a 2 M NaOH solution. Then, it was put in a Teflon®-lined stainless-steel autoclave (V_{total} = 623 mL; V_{fill}/V_{total} = 29%). This was followed by hydrothermal treatment at 180 °C for 12 h. The resulting carbon spheres were then purified with acetone by centrifugation in three cycles. After drying at 40 °C, the solid product was collected and ground in an agate mortar.

Second, for the preparation of hollow TiO_2 spheres, 0.1 g of carbon spheres were added to 20 mL of absolute ethanol under vigorous stirring. Then, 1 mL of titanium(IV) butoxide was added dropwise at a rate of 1 mL•min^{-1} to the suspension. After drying, the obtained powder (~400 mg) was placed in a ceramic boat to eliminate the templates *via* calcination in a Thermolyne 21,100 tube furnace at 500 °C for 3 h applying a heating rate of 5 °C•min^{-1} under constant air supply (~30 L•h^{-1}). Finally, the solid product was collected and ground in an agate mortar. A reference TiO_2 sample was also synthesized the same way as described in this paragraph, just without the addition of carbon spheres.

Third, for the preparation of hollow ZnO spheres, 0.3 g of carbon spheres and 3.4 g of zinc acetylacetonate were added to a mixture of 194.6 mL of absolute ethanol and 1.372 mL of Milli-Q water and stirred for 1 h. Then, this was transferred to a Teflon®-lined stainless-steel autoclave (V_{total} = 280 mL; V_{fill}/V_{total} = 70%) and the solvothermal treatment was carried out at 180 °C for 12 h. The resulting product was purified *via* centrifugation three times using 4×50 mL centrifugation tubes and a mixture of ethanol and Milli-Q water (V/V% = 65, 45, 20% for the first, second and third cycles, respectively). After drying, the solid powder was put into a ceramic boat, and the carbon spheres were eliminated using the same parameters as described in the previous paragraph. For this purpose, approximately 400 mg of solid powder was used in this case as well, to ensure the complete elimination of the templates. Finally, the solid product was collected and ground in an agate mortar.

Fourth, the immobilization of photocatalysts was carried out using ceramic papers (10×17 cm) that were wetted with ethanol. Then, the papers were dipped in a 1:2 (V/V) mixture of isopropyl alcohol and titanium(IV) isopropoxide. After that, they were spray coated with photocatalysts (m = 1 g) previously suspended in ethanol (V = 50 mL) *via* ultrasonication. The resulting sheets were dried for 24 h at room temperature. The amorphous titanium oxide hydroxide formed as a result of these steps ensured the immobilization of the photocatalysts. Lastly, the coated ceramic papers were illuminated with UV light (λ_{max} = 365 nm) for 24 h to eliminate any possible residual volatile compounds and organic matter. More details regarding these syntheses and immobilization technique can be found in our previous publications [15–17,26].

The samples prepared in this work were denoted as follows: “CP” stands for “ceramic paper”, “ref” stands for “reference” (i.e., non-hollow solid spheres) and “HS” stands for “hollow sphere”. The “CP_blank” name refers to the ceramic paper containing titanium oxide hydroxide formed as a result of the hydrolysis of titanium(IV) isopropoxide adhesive.

2.3. Characterization methods and instrumentation

X-ray powder diffraction (XRD) measurements were carried out with a Rigaku Miniflex II diffractometer to determine the crystalline composition of the samples using the following parameters: $\lambda_{Cu\ K\alpha}$ = 0.15406 nm, 30 mA and 40 kV, 20–40 (2θ°) region for TiO_2 and ZnO and 20–70 (2θ°) for the ceramic paper-containing samples. Scanning electron microscopy (SEM) measurements were performed with a Hitachi S-4700 Type II microscope applying 10 kV acceleration voltage to investigate the general morphology of the samples. Transmission electron microscopy (TEM) measurements were carried out with a FEI Tecnai G^2 20 X-Twin microscope to investigate the hollow structure of the catalysts. Fourier transform infrared spectroscopy (FTIR) measurements were taken with a Jasco 6200 spectrometer in the 400–4000 cm^{-1} range applying 4 cm^{-1} spectral resolution to identify the functional groups in the samples. Specific surface areas were determined with a BELCAT-A device *via* nitrogen adsorption at 77 K using the Brunauer-Emmett-Teller (BET) method. To investigate the stability of the photocatalysts, XRD and SEM measurements were repeated following the photocatalytic activity measurements.

2.4. Photocatalytic activity, stability and reusability measurements

The photocatalytic activities of both suspended and immobilized catalysts were evaluated by using phenol as a pollutant (c = 0.1 mM) under UV-A (λ = 365 nm) light irradiation. In the former case, the catalysts (m = 100 mg) were suspended in 100 mL of phenol-containing water and placed in a glass vessel surrounded by six UV fluorescent tubes (Vilber-Lourmat T-6L, UV-A, 6 W). During these 4-hour-long

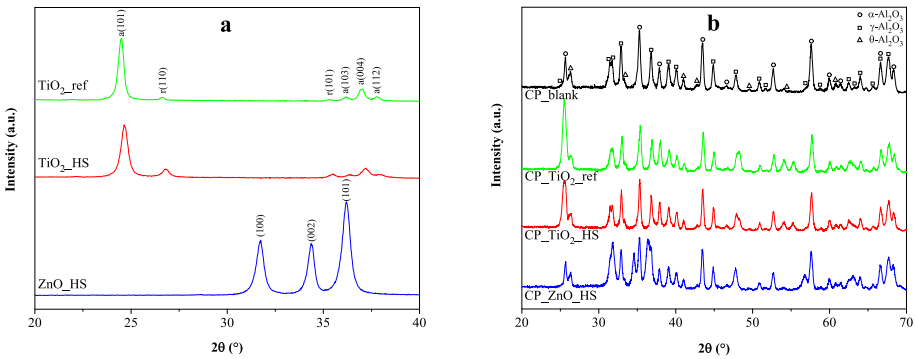

Fig. 1. XRD patterns of (a) non-immobilized and (b) immobilized photocatalysts.

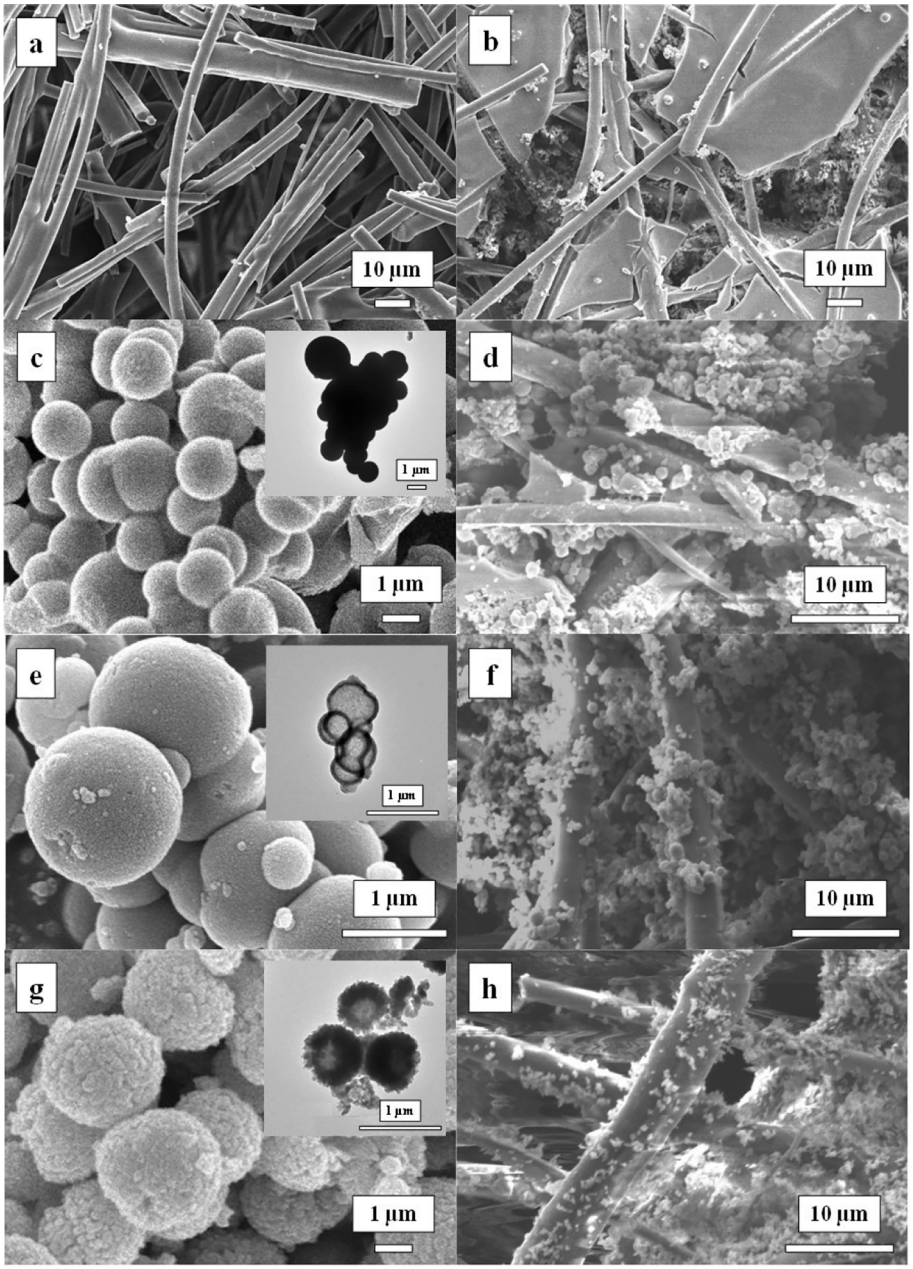

Fig. 2. SEM micrographs of (a) ceramic paper, (b) ceramic paper with hydrolyzed adhesive, (c) solid TiO_2 spheres (inset: corresponding TEM image) used as a reference, (d) solid TiO_2 spheres immobilized on ceramic paper, (e) hollow TiO_2 spheres (inset: corresponding TEM image), (f) hollow TiO_2 spheres immobilized on ceramic paper, (g) hollow ZnO spheres (inset: corresponding TEM image), and (h) hollow ZnO spheres immobilized on ceramic paper.

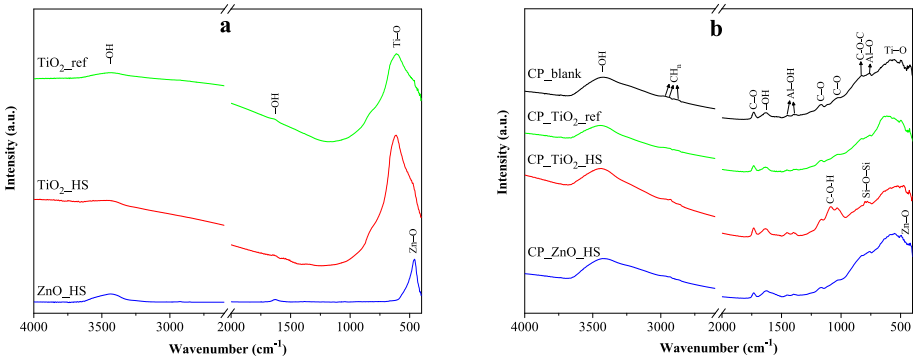

Fig. 3. FTIR spectra of TiO_2 and ZnO samples (a) before and (b) after their immobilization on ceramic paper.

measurements constant magnetic stirring, temperature (25 °C) and air supply were provided. For the investigation of immobilized catalysts, the ceramic paper containing them was locked on the top of a fixed bed flow reactor. The top part of this reactor was tilted at an angle of 10°. The water to be treated (V = 600 mL) containing phenol was constantly recirculated with a centrifugal pump (3.5 L•min^{-1}). The excitation of immobilized catalysts was carried out with three UV fluorescent tubes (Lightech, UV-A, 40 W) placed above the reactor (irradiation height = 15 cm). To investigate the reusability of both suspended and immobilized catalysts, the phenol degradation experiments were repeated two additional times for each sample. The concentration of phenol was measured by high performance liquid chromatography. The device applied was an Agilent 1290 Infinity II that consisted of a binary pump and a diode array detector ($\lambda_{detection}$ = 210 nm). A Poroshell 120 C18 column was used as the stationary phase containing particles with a diameter of 2.7 μm. As eluent, an 80:20 (V/V) mixture of methanol and water was used with a flow rate of 1 mL•min^{-1}.

3. Results and discussion

3.1. Characterization

Before carrying out the immobilization of photocatalysts (m_0 = 1 g), the weights of the following were measured: ceramic paper, ceramic paper containing the adhesive (i.e., hydrolyzed titanium oxide hydroxide), and ceramic paper containing both the adhesive and photocatalysts. The purpose of this was to calculate the amount of immobilized catalysts and the coverage of the ceramic paper. Accordingly, 1.14, 1.16 and 2.05 mg•cm^{-2} coverages were measured for CP_TiO_2_ref, CP_TiO_2_HS and CP_ZnO_HS (equivalent to $m_{immobilized}$ = 0.194, 0.198 and 0.353 g weights), respectively. This result is in good agreement with the observation that a more stable suspension could be prepared from ZnO_HS than from TiO_2_ref and TiO_2_HS. During the immobilization process it was found that only those catalysts that were spray coated as a stable suspension attached well to the surface. Hence, during this process, the catalyst suspensions were subjected to constant ultrasonication. Due to the low relative ratio of catalyst weight to ceramic paper weight (m_{CP} = 3.217 g), it was expected that the features of ceramic paper will dominate those of the catalysts during characterization. Therefore, the results will be presented both in the presence and absence of the support. Finally, the TiO_2_ref and TiO_2_HS samples have already been characterized in our previous publication in detail [26], but for the sake of easy comparability they will also be shown and summarized briefly.

3.1.1. XRD measurements

The XRD patterns are summarized in Fig. 1. Based on Fig. 1a it was ascertained that TiO_2_ref and TiO_2_HS consisted of predominantly anatase (24.7 2θ°), but they contained some rutile (26.9 2θ°) as well [36]. The primary crystallite size of the former was D = 35 nm, while that of the latter was D = 26.5 nm. The reflections at 31.7, 34.4 and 36.2 2θ° in ZnO_HS were attributed to ZnO wurtzite structure [37] that had a primary crystallite size of D = 26.2 nm. Despite the relatively low crystallite sizes of the samples, their specific surface areas were very low (<6 m^2•g^{-1} in all cases). Prior their immobilization on ceramic paper, the XRD pattern of CP_blank was recorded, which was rather complex (Fig. 1b). It was found that the support consisted of α-Al_2O_3, γ-Al_2O_3 and θ-Al_2O_3 based on the COD cards No. 1000032, 1,200,005 and 4002418, respectively. The most intense diffraction peaks of both TiO_2 and ZnO overlap with those of Al_2O_3, making the detection of the formers challenging. However, the peak areas of these corresponding reflections in CP_TiO_2_ref, CP_TiO_2_HS and CP_ZnO_HS were always found to be significantly higher than those in CP_blank. This finding is also observable in Fig. 1b based on the intensity or full width at half maximum values. These results give indirect evidence of the successfulness of the immobilization process.

To further support the coverage values obtained from the weight measurements, the following steps were taken. The well-known TiO_2 reference, Aeroxide P25 was used as an internal standard. Accordingly, mixtures of known P25:CP weight ratios were prepared. These samples (together with CP_blank, CP_TiO_2_ref, CP_TiO_2_HS and CP_ZnO_HS) were calcined at 1000 °C for 5 h. This approach has numerous advantages: i) the main component of ceramic paper, α-Al_2O_3 is resistant to structural changes at this temperature, therefore it remained unchanged; ii) the TiO_2 content of each sample transformed into thermodynamically stable rutile, making the calculations simpler; iii) due to the high temperature, the crystallinity of the samples increased, enhancing the signal to noise ratio. As the next step, a calibration curve was prepared (Fig. S1), based on which solely the immobilized TiO_2 and ZnO contents could be determined. The coverage values obtained using this method (1.08, 1.01 and 2.29 mg•cm^{-2} coverages were calculated for CP_TiO_2_ref, CP_TiO_2_HS and CP_ZnO_HS, respectively) were in a reasonably good agreement with the ones obtained from the weight measurements.

3.1.2. SEM and TEM measurements

The results of morphological measurements are shown in Fig. 2. Based on Fig. 2a, the blank ceramic paper, which was used as a support, consisted of uncoated Al_2O_3 fibers. After the addition of titanium(IV) isopropoxide followed by its hydrolysis during drying, amorphous titanium oxide hydroxide was formed (CP_blank; Fig. 2b). This is represented by the slabs surrounding the uncoated Al_2O_3 fibers. Fig. 2c shows a SEM image of the solid TiO_2 spheres (TiO_2_ref; d_{mean} = 910 nm), while in the inset, the TEM image of the same sample reinforces that the spheres were indeed non-hollow. After spray coating, TiO_2_ref partly covered and surrounded the fibers (CP_TiO_2_ref; Fig. 2d) proving the successfulness of immobilization. Fig. 2e demonstrates that TiO_2_HS (d_{mean} = 1161 nm) consisted of well-defined spheres with regular hollow cavities (Fig. 2e inset). This sample was also fixed successfully on ceramic paper (CP_TiO_2_HS; Fig. 2f). Similar conclusions were drawn for

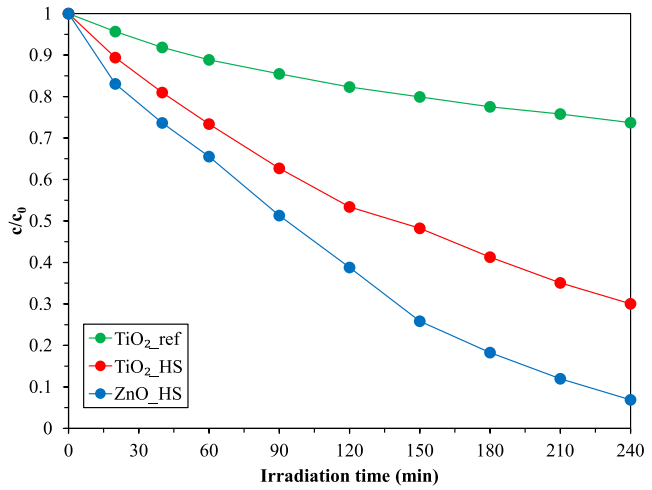

Fig. 4. Decay curves of phenol under UV irradiation for suspended photocatalysts.

ZnO_HS (d_{mean} = 800 nm; Fig. 2g) immobilized on the support (CP_ZnO_HS; Fig. 2h).

3.1.3. IR measurements

The results of FTIR measurements are shown in Fig. 3. In Fig. 3a the bands at ~3400 cm^{-1} and 1630 cm^{-1} in all of the non-immobilized samples were attributed to the stretching and bending vibrations of surface OH groups [38,39]. The broad band centered at ~615 cm^{-1} in TiO_2_ref and TiO_2_HS could be ascribed to the transverse optical vibrations of Ti–O bonds [40], while the one at 460 cm^{-1} in ZnO_HS to the stretching vibrations of Zn–O bonds [41]. The FTIR spectra of these samples were also recorded after their immobilization on ceramic paper (Fig. 3b). The support was an alumina-based Si-containing ceramic paper, whose structure was linked by an epoxy resin [16]. Due to the former, bands at 1459 and 1382 cm^{-1} could be detected representing the asymmetric stretching vibrations of Al–OH bonds [42], while the one at 759 cm^{-1} could be ascribed to Al–O stretching modes [43]. The bands at 1108, 798 and 779 cm^{-1} could be associated with Si–O–Si asymmetric stretching bonds in quartz [44–46]. Due to the epoxy resin, bands at 2984, 2930 and 2870 cm^{-1} were observed representing the stretching vibrations of CH_n bonds; the ones at 1737, 1170 and 1031 cm^{-1} indicate the presence of organic C–O bonds, while the one at 825 cm^{-1} was attributed to C–O–C stretching vibrations [47,48]. An additional band was detected in CP_TiO_2_HS at 1086 cm^{-1} that was ascribed to C–O–H vibrations in sugar moiety [48], presumably originating from the sucrose used for the synthesis. The broad band between ~450–650 cm^{-1} could be associated with Ti–O bonds [40,49–51]. This band appeared not only in CP_blank but in each sample as well, due to the presence of amorphous titanium oxide hydroxide originating from the adhesive. Based on these results no clear evidence could be found regarding the formation of a chemical interaction between the support and catalysts. However, it is worth mentioning that the existence of one cannot be excluded solely based on the absence of notable shifts in the Al–O(H) and Ti–O band positions.

3.2. Photocatalytic activity measurements

The photocatalytic activity of the samples was evaluated *via* the photocatalytic oxidation of phenol. First, the catalysts were applied as a suspension (Fig. 4), ensuring the highest possible contact area between the catalysts and the pollutant. It was ascertained that compared to the reference catalyst containing non-hollow solid spheres, the hollow ones were notably more efficient. TiO_2_ref reduced the concentration of phenol by 26%, while this value was 70% for TiO_2_HS and 93% for ZnO_HS. In our previous publication this was attributed to the enhanced visible light harvesting capability of the hollow catalysts, due to the higher probability of incident light waves constructively interfering with each other [26]. During the degradation of phenol, the formation of hydroquinone was observed as a byproduct and no significant differences were observed in the amounts and evolution trends (Fig. S2).

Second, the reusability and stability of the catalysts were

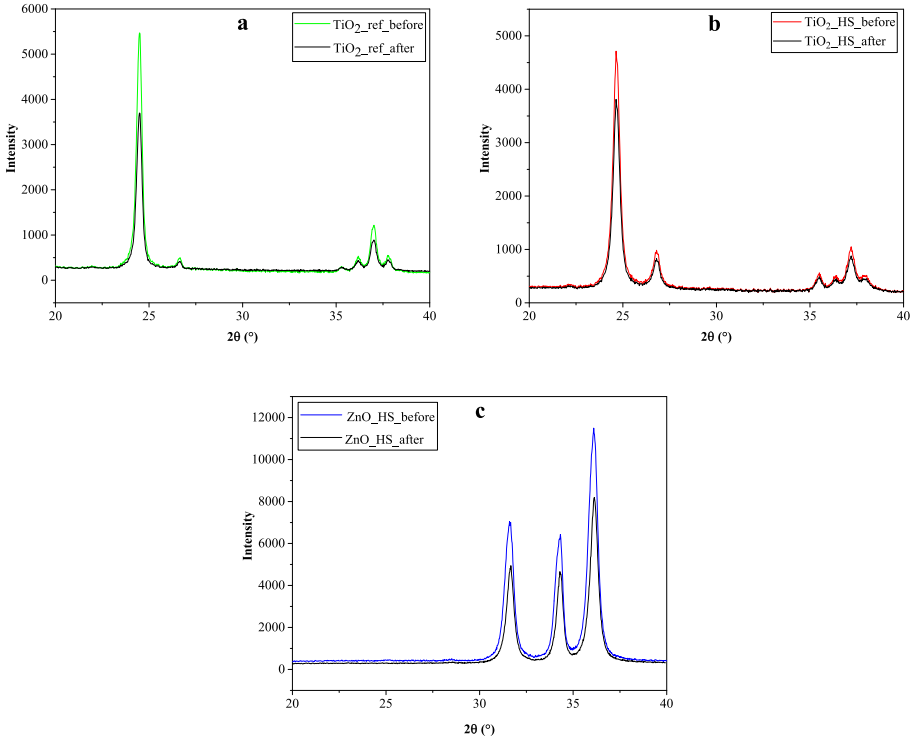

Fig. 5. XRD patterns of photocatalysts before and after phenol degradation experiments for (a) TiO_2_ref, (b) TiO_2_HS and (c) ZnO_HS.

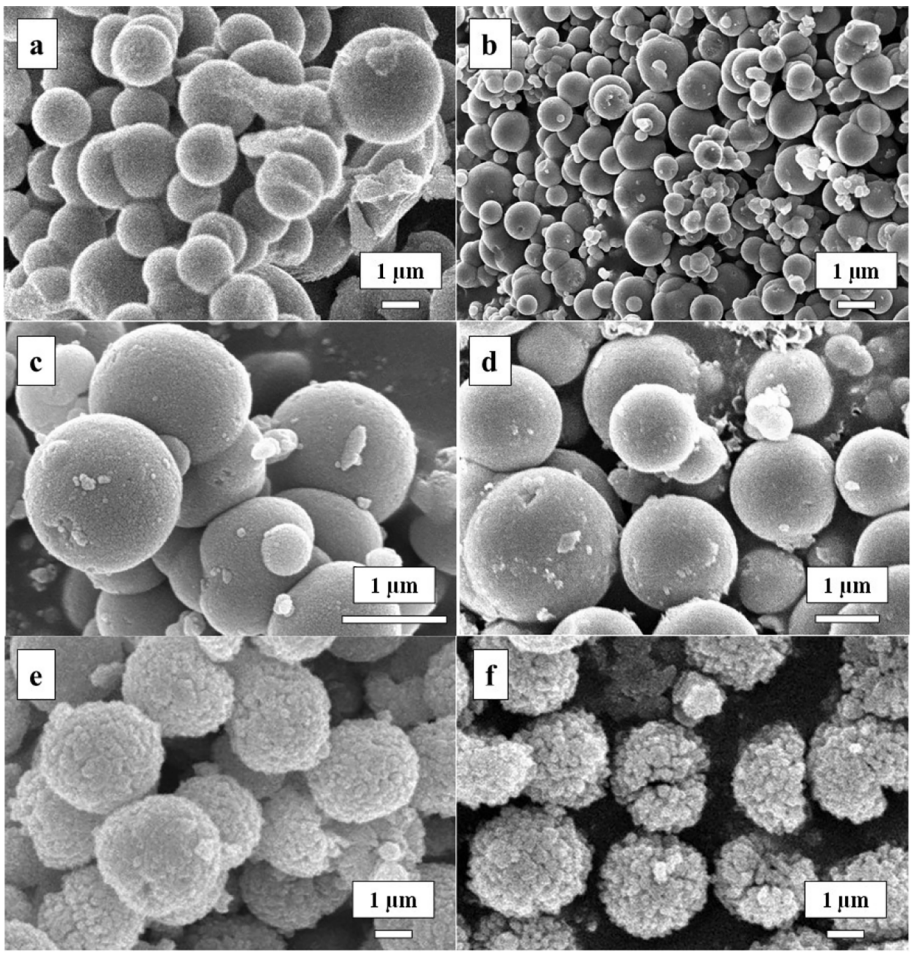

Fig. 6. SEM micrographs of photocatalysts before and after phenol degradation experiments for (a, b) TiO_2_ref, (c, d) TiO_2_HS and (e, f) ZnO_HS, respectively.

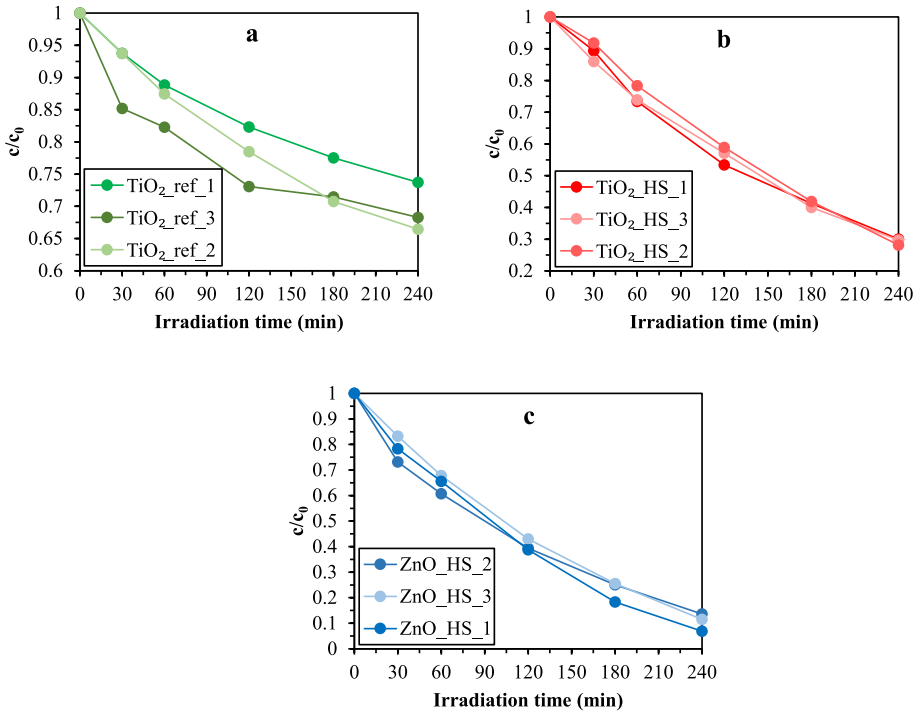

Fig. 7. Decay curves of phenol obtained following reusability experiments for (a) TiO_2_ref, (b) TiO_2_HS and (c) ZnO_HS.

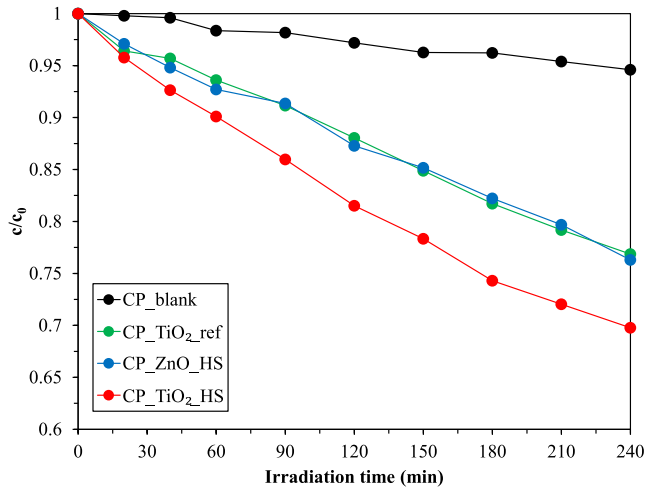

Fig. 8. Decay curves of phenol under UV irradiation for immobilized photocatalysts.

investigated. For the former, phenol degradation experiments were carried out three times, while for the latter, XRD and SEM measurements were repeated after the photoactivity measurements. The catalysts proved to be stable as they completely retained their crystal phase composition (Fig. 5) and morphology (Fig. 6) as well. The words "before" and "after" at the end of sample names indicate whether the measurements were carried out before or after the phenol degradation experiments, respectively. The catalysts were found to be remarkably reusable, as they largely retained their photocatalytic activity even after three consecutive phenol degradation measurements (Fig. 7). The number after each sample indicate in what order the consecutive phenol degradation experiments were carried out.

Third, the catalysts were immobilized on ceramic paper to investigate their practical applicability, and the results of phenol degradation are shown in Fig. 8. Titanium(IV) isopropoxide was used as an adhesive that interacted with the moisture in air during drying, resulting in amorphous titanium oxide hydroxide on the support (CP_blank). Amorphous TiO_2 is known to be rather inactive due to the facilitated recombination of photogenerated electron–hole pairs [52,53]. Still, the photocatalytic activity of CP_blank was also investigated, which was found to be very low (~5% degraded phenol), as expected. Then, it was ascertained that the observed photocatalytic activity order was reversed as follows. The efficiency of ZnO_HS was higher than that of TiO_2_HS, but after immobilization, despite the smaller coverage of CP_TiO_2_HS compared to that of CP_ZnO_HS, it was still more efficient. A plausible explanation for this could be the following. On the ceramic paper, the catalysts and the adhesive came into close contact due to the immobilization process. The presence of crystalline TiO_2 on amorphous TiO_2 could result in seed induced crystallization [54]. Consequently, between the adhesive (i.e., amorphous TiO_2 underway to be crystallized) and the samples a heterojunction was formed. The distance in energy between the conduction bands of TiO_2 from the adhesive and crystalline TiO_2 hollow spheres is significantly lower [34] than that between TiO_2 from the adhesive and ZnO [55]. This means that the occurrence of electron transfer between the corresponding conduction bands are much more probable in the former case than that in the latter case. As a result, CP_TiO_2_HS could be excited more efficiently than CP_ZnO_HS, presumably leading to more efficient free radical generation and ultimately, higher photocatalytic activity. It is also plausible that crystalline TiO_2 hollow spheres are more likely to initiate the crystallization of amorphous TiO_2 (due to them having similar crystallographic parameters; tetragonal structure) than crystalline ZnO hollow spheres (wurtzite-like hexagonal structure).

Fourth, the reusability of immobilized catalysts was also investigated. These results for CP_blank, CP_TiO_2_ref, CP_TiO_2_HS and

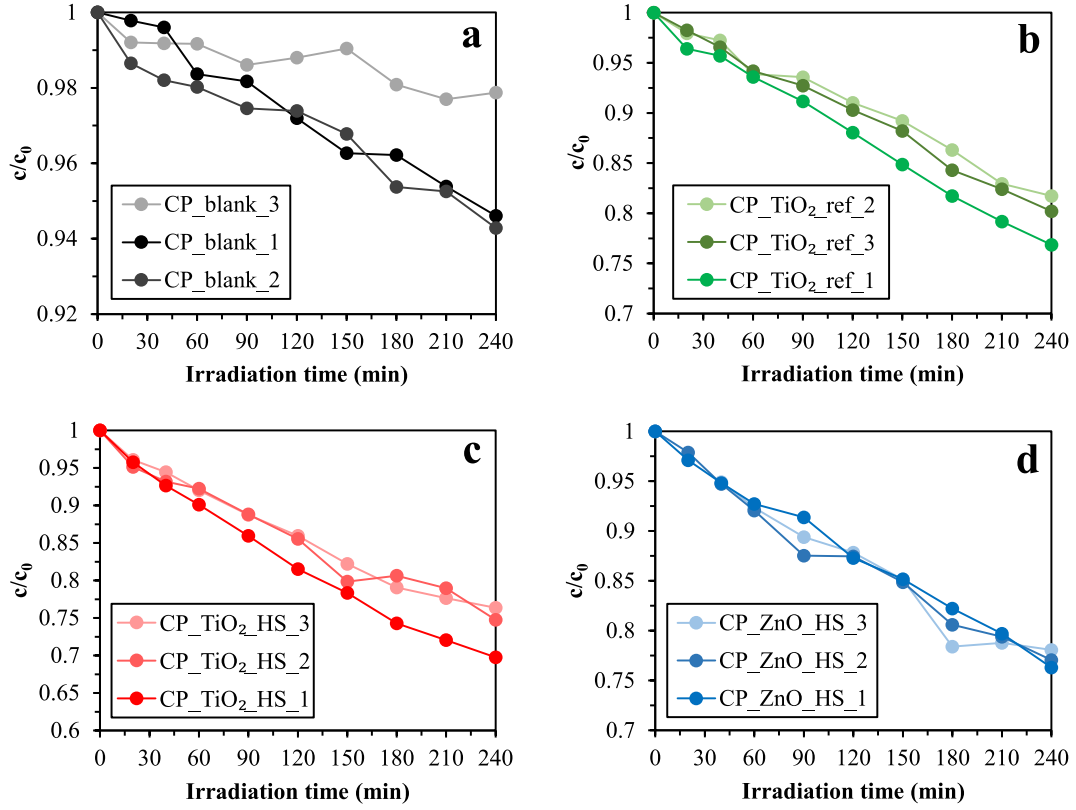

Fig. 9. Decay curves of phenol under UV irradiation measured during reusability and stability experiments for (a) ceramic paper with adhesive (b) solid TiO_2 spheres, (c) hollow TiO_2 spheres, and (d) hollow ZnO spheres.

CP_ZnO_HS are shown in Fig. 9a–d, respectively. All of the samples were found to be reasonably reusable: the maximum difference observed in degraded phenol amount was 6% (for CP_TiO_2_HS) after three measurements. During this period no photocatalyst leaching was observed, demonstrating that the samples were remarkably stable, and that the immobilization process was successful.

4. Conclusions

TiO_2 and ZnO photocatalysts of hollow sphere morphology were successfully prepared (together with a solid TiO_2 sphere reference), which was reinforced by SEM and TEM measurements. Following their immobilization on ceramic paper, 1.14, 1.16 and 2.05 mg•cm^{-2} coverages were calculated for CP_TiO_2_ref, CP_TiO_2_HS and CP_ZnO_HS, respectively. The presence of catalysts on the support was supported not only by SEM, but by XRD and IR measurements as well. Suspended TiO_2_ref, TiO_2_HS and ZnO_HS reduced the concentrations of phenol by 26, 70 and 93%, which values were higher than those calculated for their immobilized counterparts. After immobilization, the efficiency of CP_TiO_2_HS was higher than that of CP_ZnO_HS, although this order was reversed when they were applied as suspensions. This was explained by the formation of a heterojunction, resulting in the more efficient excitation of CP_TiO_2_HS. The immobilized catalysts were proved to be remarkably stable, as they largely retained their photocatalytic activity after three consecutive phenol degradation measurements.

CRediT authorship contribution statement

Tamás Gyulavári: Writing – review & editing, Writing – original draft, Investigation, Conceptualization. **Viktória Márta:** Investigation. **Zoltán Kovács:** Conceptualization, Investigation. **Klára Magyari:** Investigation. **Zsolt Kása:** Investigation. **Gábor Veréb:** Writing – review & editing. **Zsolt Pap:** Supervision, Writing – original draft. **Klara Hernadi:** Writing – review & editing, Funding acquisition.

Declaration of Competing Interest

The authors declare that they have no known competing financial interests or personal relationships that could have appeared to influence the work reported in this paper.

Acknowledgements

This study was financed by the NKFI-K-124212 project. T. Gyulavári is grateful for the financial support of the NKFI-TNN-16-123631 project. Zs. Pap and K. Magyari acknowledges the Bolyai János scholarship provided by the Hungarian Academy of Sciences. Zs. Kása is grateful for the National Research Development and Innovation Office for the financial support (Grant number: GINOP-2.3.4-15-2020-00006).

References

[1] V.M. Joy, S. Dutta, S. Feroz, G. Devi, Nanophotocatalytic treatment of seawater using TiO_2 immobilized and suspension system under solar irradiation, J. Water Proc. Eng. 43 (2021), 102263, https://doi.org/10.1016/j.jwpe.2021.102263.
[2] D. Camacho-Munoz, A.S. Fervers, C.J. Pestana, C. Edwards, L.A. Lawton, Degradation of microcystin-LR and cylindrospermopsin by continuous flow UV-A photocatalysis over immobilised TiO_2, J. Environ. Manage. 276 (2020), 111368, https://doi.org/10.1016/j.jenvman.2020.111368.
[3] V.G. Bessergenev, M.C. Mateus, I.M. Morgado, M. Hantusch, E. Burkel, Photocatalytic reactor, CVD technology of its preparation and water purification from pharmaceutical drugs and agricultural pesticides, Chem. Eng. J. 312 (2017) 306–316, https://doi.org/10.1016/j.cej.2016.11.148.
[4] N. Liu, J. Ming, A. Sharma, X. Sun, N. Kawazoe, G. Chen, Y. Yang, Sustainable photocatalytic disinfection of four representative pathogenic bacteria isolated from real water environment by immobilized TiO_2-based composite and its mechanism, Chem. Eng. J. 426 (2021), 131217, https://doi.org/10.1016/j.cej.2021.131217.
[5] A. Bouarioua, M. Zerdaoui, Photocatalytic activities of TiO_2 layers immobilized on glass substrates by dip-coating technique toward the decolorization of methyl orange as a model organic pollutant, J. Environ. Chem. Eng. 5 (2) (2017) 1565–1574, https://doi.org/10.1016/j.jece.2017.02.025.
[6] V. Píšťková, M. Tasbihi, M. Vávrová, U.L. Štangar, Photocatalytic degradation of β-blockers by using immobilized titania/silica on glass slides, J. Photochem. Photobiol. A Chem. 305 (2015) 19–28, https://doi.org/10.1016/j.jphotochem.2015.02.014.
[7] M. Gar Alalm, M. Samy, S. Ookawara, T. Ohno, Immobilization of S-TiO_2 on reusable aluminum plates by polysiloxane for photocatalytic degradation of 2,4-dichlorophenol in water, J. Water Proc. Eng. 26 (2018) 329–335, https://doi.org/10.1016/j.jwpe.2018.11.001.
[8] M. Tasbihi, M. Kete, A.M. Raichur, N.N. Tusar, U.L. Stangar, Photocatalytic degradation of gaseous toluene by using immobilized titania/silica on aluminum sheets, Environ. Sci. Pollut. Res. Int. 19 (9) (2012) 3735–3742, https://doi.org/10.1007/s11356-012-0864-6.
[9] S. Chandra Pragada, A.K. Thalla, Polymer-based immobilized Fe2O3-TiO2/PVP catalyst preparation method and the degradation of triclosan in treated greywater effluent by solar photocatalysis, J. Environ. Manage. 296 (2021) 113305. 10.1016/j.jenvman.2021.113305.
[10] O. Ounas, B. Lekhlif, J. Jamal-eddine, The facile immobilization of ZnO into a polymer surface for photodegradation of organic contaminants, Mater. Today: Proceedings 30 (2020) 816–822, https://doi.org/10.1016/j.matpr.2020.04.179.
[11] O. Ounas, A.A. El Foulani, B. Lekhlif, J. Jamal-Eddine, Immobilization of TiO_2 into a poly methyl methacrylate (PMMA) as hybrid film for photocatalytic degradation of methylene blue, Mat. Today: Proceedings 22 (2020) 35–40, https://doi.org/10.1016/j.matpr.2019.08.068.
[12] V.S. Kosera, T.M. Cruz, E.S. Chaves, E.R.L. Tiburtius, Triclosan degradation by heterogeneous photocatalysis using ZnO immobilized in biopolymer as catalyst, J. Photochem. Photobiol. A Chem. 344 (2017) 184–191, https://doi.org/10.1016/j.jphotochem.2017.05.014.
[13] H. Mahdizadeh, A. Nasiri, M.A. Gharaghani, G. Yazdanpanah, Hybrid UV/COP advanced oxidation process using ZnO as a catalyst immobilized on a stone surface for degradation of acid red 18 dye, MethodsX 7 (2020), 101118, https://doi.org/10.1016/j.mex.2020.101118.
[14] G. Du, P. Feng, X. Cheng, J. Li, X. Luo, Immobilizing of ZIF-8 derived ZnO with controllable morphologies on zeolite A for efficient photocatalysis, J. Solid State Chem. 255 (2017) 215–218, https://doi.org/10.1016/j.jssc.2017.07.035.
[15] G. Simon, T. Gyulavári, K. Hernádi, M. Molnár, Z. Pap, G. Veréb, K. Schrantz, M. Náfrádi, T. Alapi, Photocatalytic ozonation of monuron over suspended and immobilized TiO_2 –study of transformation, mineralization and economic feasibility, J. Photochem. Photobiol. A Chem. 356 (2018) 512–520, https://doi.org/10.1016/j.jphotochem.2018.01.025.
[16] Z. Kasa, E. Orban, Z. Pap, I. Abraham, K. Magyari, S. Garg, K. Hernadi, Innovative and Cost-Efficient BiOI Immobilization Technique on Ceramic Paper-Total Coverage and High Photocatalytic Activity, Nanomater. 10 (10) (2020), https://doi.org/10.3390/nano10101959.
[17] G. Veréb, Z. Ambrus, Z. Pap, K. Mogyorósi, A. Dombi, K. Hernádi, Immobilization of crystallized photocatalysts on ceramic paper by titanium(IV) ethoxide and photocatalytic decomposition of phenol, React. Kinet. Mech. Catal. 113 (1) (2014) 293–303, https://doi.org/10.1007/s11144-014-0734-y.
[18] P. Hegedűs, E. Szabó-Bárdos, O. Horváth, P. Szabó, K. Horváth, Investigation of a TiO_2 photocatalyst immobilized with poly(vinyl alcohol), Catal. Today 284 (2017) 179–186, https://doi.org/10.1016/j.cattod.2016.11.050.
[19] H. Azizi-Toupkanloo, M. Karimi-Nazarabad, G.-R. Amini, A. Darroudi, Immobilization of AgCl@TiO_2 on the woven wire mesh: Sunlight-responsive environmental photocatalyst with high durability, Sol. Energy 196 (2020) 653–662, https://doi.org/10.1016/j.solener.2019.12.046.
[20] Á. Veres, J. Ménesi, Á. Juhász, O. Berkesi, N. Ábrahám, G. Bohus, A. Oszkó, G. Pótári, N. Buzás, L. Janovák, I. Dékány, Photocatalytic performance of silver-modified TiO_2 embedded in poly(ethyl-acrylate-co-methyl metacrylate) matrix, Colloid. Polym. Sci. 292 (1) (2013) 207–217, https://doi.org/10.1007/s00396-013-3063-1.
[21] J. Le Cunff, V. Tomašić, O. Wittine, Photocatalytic degradation of the herbicide terbuthylazine: Preparation, characterization and photoactivity of the immobilized thin layer of TiO_2/chitosan, J. Photochem. Photobiol. A Chem. 309 (2015) 22–29, https://doi.org/10.1016/j.jphotochem.2015.04.021.
[22] G. Balasubramanian, D. Dionysiou, M. Suidan, I. Baudin, J. Laine, Evaluating the activities of immobilized TiO2 powder films for the photocatalytic degradation of organic contaminants in water, Appl. Catal. B Environ. 47 (2) (2004) 73–84, https://doi.org/10.1016/j.apcatb.2003.04.002.
[23] M.C. Wu, J. Hiltunen, A. Sapi, A. Avila, W. Larsson, H.C. Liao, M. Huuhtanen, G. Toth, A. Shchukarev, N. Laufer, A. Kukovecz, Z. Konya, J.P. Mikkola, R. Keiski, W.F. Su, Y.F. Chen, H. Jantunen, P.M. Ajayan, R. Vajtai, K. Kordas, Nitrogen-doped anatase nanofibers decorated with noble metal nanoparticles for photocatalytic production of hydrogen, ACS Nano 5 (6) (2011) 5025–5030, https://doi.org/10.1021/nn201111j.
[24] Y. Zou, J.-W. Shi, D. Ma, Z. Fan, L. Lu, C. Niu, In situ synthesis of C-doped TiO_2@g-C_3N_4 core-shell hollow nanospheres with enhanced visible-light photocatalytic activity for H_2 evolution, Chem. Eng. J. 322 (2017) 435–444, https://doi.org/10.1016/j.cej.2017.04.056.
[25] Z.-R. Tóth, G. Kovács, K. Hernádi, L. Baia, Z. Pap, The investigation of the photocatalytic efficiency of spherical gold nanocages/TiO_2 and silver nanospheres/TiO_2 composites, Sep. Purif. Technol. 183 (2017) 216–225, https://doi.org/10.1016/j.seppur.2017.03.065.
[26] T. Gyulavári, K. Kovács, Z. Kovács, E. Bárdos, G. Kovács, K. Baán, K. Magyari, G. Veréb, Z. Pap, K. Hernadi, Preparation and characterization of noble metal modified titanium dioxide hollow spheres – new insights concerning the light

trapping efficiency, Appl. Surf. Sci. 534 (2020), 147327, https://doi.org/10.1016/j.apsusc.2020.147327.
[27] Z. Youssef, L. Colombeau, N. Yesmurzayeva, F. Baros, R. Vanderesse, T. Hamieh, J. Toufaily, C. Frochot, T. Roques-Carmes, S. Acherar, Dye-sensitized nanoparticles for heterogeneous photocatalysis: Cases studies with TiO2, ZnO, fullerene and graphene for water purification, Dyes and Pigments 159 (2018) 49–71, https://doi.org/10.1016/j.dyepig.2018.06.002.
[28] E. Savinkina, L. Obolenskaya, G. Kuzmicheva, Efficiency of sensitizing nano-titania with organic dyes and peroxo complexes, Appl. Nanosci. 5 (1) (2014) 125–133, https://doi.org/10.1007/s13204-014-0299-0.
[29] N.O. Balayeva, M. Fleisch, D.W. Bahnemann, Surface-grafted WO_3/TiO_2 photocatalysts: Enhanced visible-light activity towards indoor air purification, Catal. Today 313 (2018) 63–71, https://doi.org/10.1016/j.cattod.2017.12.008.
[30] R. Wang, M. Shi, F. Xu, Y. Qiu, P. Zhang, K. Shen, Q. Zhao, J. Yu, Y. Zhang, Graphdiyne-modified TiO_2 nanofibers with osteoinductive and enhanced photocatalytic antibacterial activities to prevent implant infection, Nat. Commun. 11 (1) (2020) 4465, https://doi.org/10.1038/s41467-020-18267-1.
[31] Y. Bao, R. Guo, M. Gao, Q. Kang, J. Ma, Morphology control of 3D hierarchical urchin-like hollow SiO_2@TiO_2 spheres for photocatalytic degradation: Influence of calcination temperature, J. Alloys Compd. 853 (2021) 157202, https://doi.org/10.1016/j.jallcom.2020.157202.
[32] E.-Z. Kedves, Z. Pap, K. Hernadi, L. Baia, Significance of the surface and bulk features of hierarchical TiO_2 in their photocatalytic properties, Ceram. Int. 47 (5) (2021) 7088–7100, https://doi.org/10.1016/j.ceramint.2020.11.061.
[33] H. Li, Z. Bian, J. Zhu, D. Zhang, G. Li, Y. Huo, H. Li, Y. Lu, Mesoporous titania spheres with tunable chamber stucture and enhanced photocatalytic activity, J. Am. Chem. Soc. 129 (27) (2007) 8406–8407, https://doi.org/10.1021/ja072191c10.1021/ja072191c.s001.
[34] J. Lyu, L. Zhou, J. Shao, Z. Zhou, J. Gao, Y. Dong, Z. Wang, J. Li, TiO_2 hollow heterophase junction with enhanced pollutant adsorption, light harvesting, and charge separation for photocatalytic degradation of volatile organic compounds, Chem. Eng. J. 391 (2020), 123602, https://doi.org/10.1016/j.cej.2019.123602.
[35] T. Gyulavári, K. Kovács, K. Magyari, K. Baán, A. Szabó, G. Veréb, Z. Pap, K. Hernadi, Unexpected Link between the Template Purification Solvent and the Structure of Titanium Dioxide Hollow Spheres, Catalysts 11 (1) (2021) 112, https://doi.org/10.3390/catal11010112.
[36] Y. Masuda, K. Kato, Synthesis and phase transformation of TiO_2 nano-crystals in aqueous solutions, J. Ceram. Soc. Jpn. 117 (1363) (2009) 373–376, https://doi.org/10.2109/jcersj2.117.373.
[37] A. Khorsand Zak, W.H. Abd. Majid, M.E. Abrishami, R. Yousefi, X-ray analysis of ZnO nanoparticles by Williamson–Hall and size–strain plot methods, Solid State Sci. 13(1) (2011) 251-256. 10.1016/j.solidstatesciences.2010.11.024.
[38] J. Orlikowski, B. Tryba, J. Ziebro, A.W. Morawski, J. Przepiórski, A new method for preparation of rutile phase titania photoactive under visible light, Catal. Commun. 24 (2012) 5–10, https://doi.org/10.1016/j.catcom.2012.02.027.
[39] X. Ye, C. Zheng, L. Ma, X. Huang, Microemulsion-assisted hydrothermal preparation and infrared radiation property of TiO_2 nanomaterials with tunable morphologies and crystal form, Mater. Sci. Semicond. Process. 31 (2015) 295–301, https://doi.org/10.1016/j.mssp.2014.12.019.
[40] V. Maria Vinosel, M. Asisi Janifer, S. Anand, S. Pauline, Structural and Functional Group Characterization of Nanocomposite Fe_3O_4/TiO_2 and Its Magnetic Property, Mech. Mater. Sci. Eng. (2017), https://doi.org/10.2412/mmse.36.92.83.
[41] M. Zare, K. Namratha, S. Alghamdi, Y.H.E. Mohammad, A. Hezam, M. Zare, Q. A. Drmosh, K. Byrappa, B.N. Chandrashekar, S. Ramakrishna, X. Zhang, Novel Green Biomimetic Approach for Synthesis of ZnO-Ag Nanocomposite; Antimicrobial Activity against Food-borne Pathogen, Biocompatibility and Solar Photocatalysis, Sci. Rep. 9 (1) (2019) 8303, https://doi.org/10.1038/s41598-019-44309-w.
[42] C. Tokoro, S. Suzuki, D. Haraguchi, S. Izawa, Silicate Removal in Aluminum Hydroxide Co-Precipitation Process, Materials 7 (2) (2014) 1084–1096, https://doi.org/10.3390/ma7021084.
[43] P. Padmaja, G.M. Anilkumar, P. Mukundan, G. Aruldhas, K.G.K. Warrier, Characterisation of stoichiometric sol–gel mullite by fourier transform infrared spectroscopy, Int. J. Inorg. Mater. 3 (7) (2001) 693–698, https://doi.org/10.1016/s1466-6049(01)00189-1.
[44] F. Reig, FTIR quantitative analysis of calcium carbonate (calcite) and silica (quartz) mixtures using the constant ratio method, Application to geological samples, Talanta 58 (4) (2002) 811–821, https://doi.org/10.1016/s0039-9140(02)00372-7.
[45] Y. Song, F. Zhao, Z. Li, Z. Cheng, H. Huang, M. Yang, Electrospinning preparation and anti-infrared radiation performance of silica/titanium dioxide composite nanofiber membrane, RSC Adv. 11 (39) (2021) 23901–23907, https://doi.org/10.1039/d1ra03917b.
[46] D.O. Antonov, D.P. Tambasova, A.B. Shishmakov, I.A. Kirilyuk, E.G. Kovaleva, Acidic and Electrosurface Properties of Binary TiO_2-SiO_2 Xerogels Using EPR of pH-Sensitive Nitroxides, Gels 7 (3) (2021), https://doi.org/10.3390/gels7030119.
[47] Y. Zhang, Y. Dong, L. Liu, L. Chang, B. Zhou, Q. Chi, X. Wang, High filling alumina/epoxy nanocomposite as coating layer for Fe-based amorphous powder cores with enhanced magnetic performance, J. Mater. Sci. Mater. 30 (16) (2019) 14869–14877, https://doi.org/10.1007/s10854-019-01858-0.
[48] A.C.S. Talari, M.A.G. Martinez, Z. Movasaghi, S. Rehman, I.U. Rehman, Advances in Fourier transform infrared (FTIR) spectroscopy of biological tissues, Appl. Spectrosc. Rev. 52 (5) (2016) 456–506, https://doi.org/10.1080/05704928.2016.1230863.
[49] T. Busani, R.A.B. Devine, Dielectric and infrared properties of TiO_2 films containing anatase and rutile, Semicond. Sci. Technol. 20 (8) (2005) 870–875, https://doi.org/10.1088/0268-1242/20/8/043.
[50] M.R. Ayers, A.J. Hunt, Titanium oxide aerogels prepared from titanium metal and hydrogen peroxide, Mater. Lett. 34 (3–6) (1998) 290–293, https://doi.org/10.1016/s0167-577x(97)00181-x.
[51] V. Etacheri, M.K. Seery, S.J. Hinder, S.C. Pillai, Oxygen Rich Titania: A Dopant Free, High Temperature Stable, and Visible-Light Active Anatase Photocatalyst, Adv. Funct. Mater. 21 (19) (2011) 3744–3752, https://doi.org/10.1002/adfm.201100301.
[52] T.X. Liu, F.B. Li, X.Z. Li, TiO_2 hydrosols with high activity for photocatalytic degradation of formaldehyde in a gaseous phase, J. Hazard. Mater. 152 (1) (2008) 347–355, https://doi.org/10.1016/j.jhazmat.2007.07.003.
[53] Y. Shiraishi, N. Saito, T. Hirai, Adsorption-driven photocatalytic activity of mesoporous titanium dioxide, J. Am. Chem. Soc. 127 (37) (2005) 12820–12822, https://doi.org/10.1021/ja053265s10.1021/ja053265s.s001.
[54] W.J. Tseng, S.-M. Kao, Effect of seed particles on crystallization and crystallite size of anatase TiO_2 nanocrystals by solvothermal treatment, Adv. Powder Technol. 26 (4) (2015) 1225–1229, https://doi.org/10.1016/j.apt.2015.06.004.
[55] R. Zha, R. Nadimicherla, X. Guo, Ultraviolet photocatalytic degradation of methyl orange by nanostructured TiO_2/ZnO heterojunctions, J. Mater. Chem. A 3 (12) (2015) 6565–6574, https://doi.org/10.1039/c5ta00764j.